IPN Progress Report 42-150 August 15, 2002

Analysis of Energy Consumption for Ad Hoc Wireless Sensor Networks Using a Bit-Meter-per-Joule Metric

J. L. Gao[1]

In this article, we present a system-level characterization of the energy consumption for sensor network application scenarios. We compute a power efficiency metric—average watt-per-meter—for each radio transmission and extend this local metric to find the global energy consumption. This analysis shows how overall energy consumption varies with transceiver characteristics, node density, data traffic distribution, and base-station location.

I. Introduction

Energy consumption is one of the most important performance metrics for wireless ad hoc sensor networks because it directly relates to the operational lifetime of the network. Most research efforts are focused on performance comparisons and trade-off studies between various low-energy routing and self-organization protocols, while keeping other system parameters fixed. As a result, very little has been revealed about the relationship between the aggregate energy consumption and non-protocol parameters such as node density, network coverage area, sensor traffic generation and distribution, and transceiver power characteristics. In this article, we will explore the relationship between the non-protocol parameters and the total energy consumption while adopting a very simple network layer/routing model that serves as a benchmark for preliminary performance evaluation. We believe using such a generic protocol model is suitable in the early phases of network planning and design.

In Section II, we describe the routing and transceiver power model used in our analysis. We then derive the average watt-per-meter efficiency over a single hop in Section III. In Section IV, we combine this local energy-efficiency metric with macro-scale parameters to compute the aggregate energy consumption for a sensor network. Specifically, we examine how base-station position affects the energy consumption when traffic generation is either uniformly or non-uniformly distributed; we also examine the effect of base-station mobility. In Section V, we provide a brief discussion and analysis of the asymmetric distribution of energy consumption among the sensors. In Section VI, we conclude this article with a summary of our findings and other final remarks.

---

[1] Mission and Systems Architecture Section.

The research described in this publication was carried out by the Jet Propulsion Laboratory, California Institute of Technology, under a contract with the National Aeronautics and Space Administration.

II. Models Used for Our Analysis

A. Transceiver Power Model

In our power model, we assume a certain non-zero minimum level of power will be radiated regardless of how short a link is. However, as the link distance increases, transmission power can be raised to maintain communication reliability. On the receiving side, we assume a fixed amount of power is required to capture the incoming radio signal. Therefore, the total power required for communicating over a distance r is given by

$$p(r) = \max\{p_{\min}, \beta r^{\alpha}\} + p_{rx} \tag{1}$$

The parameter α is the power index for channel path loss at the far field of the antenna; $p_{\min}$ is the minimum transmitter power; β represents the minimum transmission power required to communicate at a reference near-field distance of 1 meter; and p_{rx} is the fixed overhead for receiving data. Based on this model, for all nodes closer than $r_{p_{\min}} = (p_{\min}/\beta)^{1/\alpha}$, the power requirement is constant at $p_{\min}$ watts.

B. Node Location and Data Generation

We model the sensor distribution as a two-dimensional Poisson Field with constant mean and variance of λ nodes/m^2. Therefore, the probability distribution for the number of sensor nodes located within an area of A m^2 is given by

$$P\big(N(A) = k\big) = \frac{(\lambda A)^k}{k!} e^{-\lambda A}$$

and, within any given area, the location of each node is a uniformly distributed two-dimensional random vector.

We envision that the total volume of data generated by each sensor is dependent on its ability to observe and separate the signal generated by a phenomenon from the ambient noise. This ability will, in general, depend on the relative position between a phenomenon and the sensor itself. A suitable traffic-generation model will incorporate the location of the sensor as a parameter. In our analysis, we model the volume of sensor data generated by each sensor as $\mu(x, y)$ (bits), where (x, y) is the location of the sensor. The average traffic load, written as a function of the sensor location, is then given by the expression $\rho = \lambda \cdot \mu(x, y)$ bits/m^2.

C. Sensor Network Architecture

The trend in sensor network deployment is to drive down costs and operational risks by diversification—distributing resources and functionalities among a large number of small, low-cost, yet fairly capable sensors rather than just a few large and expensive "super nodes" [4]. Diversification raises the "dimensionality" of the data set and thus reveals a whole new dimension of information about the sensed phenomenon. Diversification also opens up a new realm of advanced signal processing techniques such as data fusion and blind beam-forming [10] that greatly expanded the application domain of sensor networks. While diversification promises new functionalities and improved performance, robustness, and economics of sensor network deployment, it shrinks the size of each sensor to the point where constraints on both energy resources and the physical dimension of the antenna make it inefficient to operate in a "star" topology—where every sensor communicates directly with the end user. This is particularly true in a remote sensing application where there is a great distance separating the sensors and the user.

One way to solve the sensor-to-user communication problem is cooperative communication [7], which extends the effective transmission range of a sensor network by coordinating the modulation, coding, power, data rates, and timing of multiple, simultaneous radio transmissions from the sensors. Another more popular solution is to move from a star topology to a multi-hop “relay” topology using special relay nodes, often called a base station. The base station is designed to be the communication gateway between the sensors and the end user, thus allowing the sensors to operate using only short-range RF communications. If the sensor-to-base station distance is short, then a star topology is locally feasible. However, as a sensor network continues to grow in size, a multi-hop relay among the sensors is necessary to connect every sensor with the base station.

In this article, we assume a sensor network under a relay architecture with a single base station, with the traffic flow predominantly from the sensors to the base station.

D. Baseline Model of Location-Aware Routing Protocols

Many of today’s advanced energy-efficient routing protocols use location information to reduce energy consumption. These include Geographical Routing [8], the Zone Routing Protocol [9], and the Most Forward Within Radius [6]; other protocols, such as Power Aware Routing [5], compute a pathwise or link-by-link power metric to derive the optimal routes. While energy minimization is the primary design driver, secondary metrics, such as scalability, robustness, and adaptivity to dynamic topology, also influenced network layer protocol.

In this analysis, we are not interested in evaluating the performance of any specific energy-efficient protocols. However, we do need a baseline model so that our analysis can serve as a benchmark for comparison with more sophisticated protocols. A good basic model should meet the following criteria:

(1) Define energy metrics in terms of the most basic and fundamental concepts.

(2) Incorporate location information in the routing decision.

(3) Use the most de-coupled and scalable approach in route computation.

The reason for making our model very simple is that frequently system performance is compared for different levels of protocol complexity (or overhead). Such complexity is generally the result of adapting to a particular scenario and its operating environment. As a higher degree of complexity is added, the protocol generally becomes more adapted and performs better. Therefore, a baseline model should start with the lowest degree of complexity.

For our baseline routing model, the decision metric is “power per meter,” defined as the power required for communicating information reliably per unit distance toward the destination node. Another equivalent metric is “joule per bit-meter,” which can be derived from the power-per-meter metric given that the data rate is known. Joule per bit-meter is defined as the energy required to forward one data unit of information reliably over one distance unit toward the destination node. Each sensor has the option of communicating with a large number of neighbors, which ideally also include the base station itself. The neighboring node whose power-per-meter metric is the optimal, i.e., the lowest, will be chosen to relay the sensor data. However, if this optimal relay happens to be farther away than the base station itself, then direct communication with the base station is preferred. Because this routing process strives to make forward progress toward the base station, all multi-hop paths are loop-free. We make two further assumptions regarding such a routing scheme: (1) the sensor nodes are location aware with respect to the base station and all sensor nodes that can provide forward progress toward the base station, and (2) the peak transmission power is unlimited—this assumption simplifies the mathematics of our analysis.

A final remark must be made regarding interference. Both the power model and our baseline routing protocol do not account for the energy cost of managing and overcoming co-channel interference. We assume that the channel-access mechanism is utilized to control interference overhead.

III. Power Efficiency over a Single Hop

In this section, we will analyze the one-hop power efficiency as measured by the power-per-meter metric. We will compute this metric over a single hop. In later sections, we will generalize it to compute the total energy consumption for a sensor network.

A. The Watt-per-Meter Metric

We define the watt-per-meter metric as the average power required to reliably move information per unit distance *toward* the eventual destination location. Figure 1 illustrates the general spatial relation when node A wishes to send data to the base station via node B. Since the data A sends to B is destined for the base station, the net forward progress, i.e., the net reduction of the distance to the base station, is given by

$$D - d(B, \text{base station}) = D - \sqrt{\left(D - r\cos(\theta)\right)^2 + \left(r\sin(\theta)\right)^2}$$

$$\simeq r\cos(\theta) \text{ when } D \gg r \tag{2}$$

For simplicity of analysis, we assume the base station is far away, i.e., D is quite large such that $r\cos(\theta)$ is a good approximation of the net forward progress. The watt-per-meter efficiency over link (A, B) with respect to the base station can now be defined as

$$\eta(r,\theta) = \frac{p(r)}{r\cos(\theta)} = \frac{\max\{p_{\min}, \beta r^{\alpha}\} + p_{rx}}{r\cos(\theta)} \tag{3}$$

For a given r, η is strictly increasing function with respect to θ in the range $(-\pi/2, \pi/2)$. For a given θ, η is decreasing function for small r because the transmitter power is constant; as distance increases, however, its power consumption will eventually grow as r^{α}, and η will be increasing function of r eventually.

Let $\eta^*(\theta)$ and $r^*(\theta)$ be the minimum watt per meter and the corresponding transmission distance at angle θ. Note that η is differentiable with respect to $r > 0$ except when $\beta r^{\alpha} = p_{\min}$, which is $r^*(\theta)$ when $p_{rx} = 0$. When $p_{rx} > 0$, $r^*(\theta)$ will increase and become a differentiable point, and can be derived by finding the root of the derivative of η with respect to r. In summary, we have

$$r^*(\theta) = \left\{ \begin{array}{ll} \left(\dfrac{p_{\min}}{\beta}\right)^{1/\alpha} & \text{when } \dfrac{p_{rx}}{\alpha - 1} < p_{\min} \\ \left(\dfrac{p_{rx}}{\beta(\alpha-1)}\right)^{1/\alpha} & \text{when } p_{rx} > 0, \dfrac{p_{rx}}{\alpha - 1} \geq p_{\min} \end{array} \right\} = r^* \tag{4}$$

and

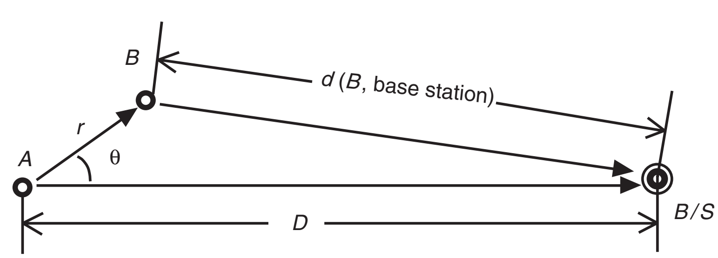

Fig. 1. Routing at distance *R* from the base station.

$$\eta^* = \eta\left(r^*, 0\right) \tag{5}$$

One will notice that since r^* is independent of θ, then

$$\eta^*\left(\theta\right) = \eta\left(r^*, \theta\right) = \frac{\eta\left(r^*, 0\right)}{\cos\left(\theta\right)} = \frac{\eta^*}{\cos\left(\theta\right)} \tag{6}$$

η^* is the optimal efficiency that can be achieved given a relay neighbor is located precisely at distance r^* and in the same direction as the base station. However, when precise control of sensor position is not possible, relay efficiency will degrade.

To achieve a watt-per-meter metric $a > \eta^*$, the maximum possible angular deviation is

$$\theta'(a) = \cos^{-1}\left(\frac{\eta^*}{a}\right) \tag{7}$$

For any relay neighbor at an angle larger than $\theta'(a)$, the watt-per-meter efficiency is strictly greater than a. For any given watt-per-meter metric a and angle $-\theta'(a) < \phi < \theta'(a)$, a relay node can be located at two possible distances, r' and r'':

$$\begin{aligned}
r'(a,\phi) &= \text{root of}\left\{\eta(r,\phi) = a, a > \eta^*, r < r^*, \phi < \theta'(a)\right\} \\
&= \begin{cases} \dfrac{p_{\min} + p_{rx}}{a\cos(\phi)}, & \text{when } a > \dfrac{p_{\min}+p_{rx}}{\cos(\phi)\left(\dfrac{p_{\min}}{\beta}\right)^{1/\alpha}} \\ \text{real root of}\left\{r^\alpha - r\dfrac{a\cos(\phi)}{\beta} + \dfrac{p_{rx}}{\beta} = 0, r < r^*, \phi < \theta'(a)\right\}, & \text{when } \dfrac{p_{\min}+p_{rx}}{\cos(\phi)\left(\dfrac{p_{\min}}{\beta}\right)^{1/\alpha}} \geq a > \eta^* \end{cases}
\end{aligned} \tag{8}$$

$$\begin{aligned}
r''(a,\phi) &= \text{root of}\left\{\eta(r,\phi) = a, a > \eta^*, r > r^*, \phi < \theta'(a)\right\} \\
&= \text{real root of}\left\{r^\alpha - r\frac{a\cos(\phi)}{\beta} + \frac{p_{rx}}{\beta} = 0, a > \eta^*, r > r^*, \phi < \theta'(a)\right\}
\end{aligned}$$

In summary, to achieve a watt-per-meter metric lower than a, a relay node's angular deviation must be less than $\theta'(a)$ in magnitude, and its distance must be bounded between $r'(a,\theta'(a))$ and $r''(a,\theta'(a))$. This defines for us a "relay zone" within which the watt-per-meter metric is less than a. We will discuss the relationship of this relay zone to the average watt per meter of a relay network in later sections. Explicit close-form solutions for r' and r'' can be found when $\alpha = 2, 3, 4$ [1].

For any chosen relay, the watt-per-meter metric is a random variable $H(D)$ that depends on the distance, R; bearing, Θ; and distance to the base station, D. Given the sensor nodes form a Poisson field, Θ will be a uniform random variable on $(-\pi/2, +\pi/2)$, and R is bounded by D. If no better relay can be found at a distance shorter than D, data will be transmitted directly to the base station.

Without loss of generality, let us consider only positive values for Θ in the range $[0, \pi/2)$. We also assume that D is at least larger then r^*. Then we can compute the distribution of $H(D)$ for a *randomly* selected relay neighbor, if available, within radius D meters:

$$
\begin{aligned}
P\big(H(D) > a\big)\big|_{a \geq \eta^*} &= P\big(H(D) > a | \Theta \leq \theta'(a)\big) P\big(\Theta \leq \theta'(a)\big) + \underbrace{P\big(H(D) > a | \Theta > \theta'(a)\big)}_{1} P\big(\Theta > \theta'(a)\big) \\
&= \int_0^{\theta'(a)} P\big(H(D) > a | \Theta = \phi\big) \cdot P_\Theta(\phi) \cdot d\phi + P\big(\Theta > \theta'(a)\big) \\
&= \frac{2}{\pi}\left[\int_0^{\theta'(a)} P\big(\big(R < r'(a,\phi)\big) \cup \big(R > \min\{r''(a,\phi), D\}\big) \big) \cdot d\phi + \Big(\frac{\pi}{2} - \theta'(a)\Big)\right] \\
&= \frac{2}{\pi}\left[\int_0^{\theta'(a)} \left(\frac{r'(a,\phi)^2}{D^2} + 1 - \frac{\min\{r''(a,\phi)^2, D^2\}}{D^2}\right) d\phi + \Big(\frac{\pi}{2} - \theta'(a)\Big)\right] \\
&= 1 - \frac{2}{\pi D^2}\int_0^{\theta'(a)} \left(\min\{r''(a,\phi)^2, D^2\} - r'(a,\phi)^2\right) d\phi \\
P\big(H(D) > a\big)\big|_{a < \eta^*} &= 1
\end{aligned}
\tag{9}
$$

But in our model, we assume that only the neighbor with the best watt-per-meter metric (i.e., the lowest H) will be selected as the relay. So we define $H^*(D)$ as the best watt-per-meter metric when the base station is at a distance D meters. The number of available relay candidates is a Poisson random variable N with mean $\lambda\pi D^2/2$ nodes/m^2. Let I be the indicator function; then we have

$$
\begin{aligned}
&P\big(H^*(D) > a\big) \\
&= \underbrace{I\big(\eta(D,0) > a\big) P(N=0)}_{\text{direct comm. with base station}} + \sum_{i=1}^{\infty} P\big(H(D) > a\big)^i P(N=i) \\
&= \sum_{i=0}^{\infty} P\big(H(D) > a\big)^i e^{-\lambda\pi D^2/2} \tfrac{(\lambda\pi D^2/2)^i}{i!} - I\big(\eta(D,0) \leq a\big) P(N=0) \\
&= \exp\left(\frac{-\lambda\pi D^2\left(1 - P\big(H(D) > a\big)\right)}{2}\right) - I\left(\beta D^{\alpha-1} \leq a\right) \exp\left(\frac{-\lambda\pi D^2}{2}\right) \\
&= \begin{cases} \exp\left(-\lambda \int_0^{\theta'(a)} \left(\min\{r''(a,\phi)^2, D^2\} - r'(a,\phi)^2\right) d\phi\right) - I\left(\beta D^{\alpha-1} \leq a\right) \exp\left(\frac{-\lambda\pi D^2}{2}\right), & \text{if } a > \eta^* \\ 1, & \text{if } a \leq \eta^* \end{cases}
\end{aligned}
\tag{10}
$$

When the base station is at the far field, we can take the limit of Eq. (10) as D approaches infinity. Then we have

$$P(H^* > a) = \lim_{D\to\infty} P\big(H^*(D) > a\big) = \begin{cases} \exp\left(-\lambda \int_0^{\theta'(a)} \left(r''(a,\phi)^2 - r'(a,\phi)^2\right) d\phi\right), & \text{if } a > \eta^* \\ 1, & \text{if } a \le \eta^* \end{cases} \tag{11}$$

Since H^* is a non-negative random variable, the expected value of the watt-per-meter metric for choosing the best relay neighbor can be computed by

$$\begin{aligned} \bar{H}^* = E[H^*] &= \int_0^\infty P(H^* > a)\, da \\ &= \eta^* + \int_{\eta^*}^\infty \exp\left(-\lambda \int_0^{\theta'(a)} \left(r''(a,\phi)^2 - r'(a,\phi)^2\right) d\phi\right) da \end{aligned} \tag{12}$$

If one knows the data rate of the radio channel, then one can calculate the bit-meter-per-joule metric for the system. Let $1/\tau$ be the transmission rate in bits per second. Then the bit-meter-per-joule metric is simply given by $\left(\tau \cdot \bar{H}^*\right)^{-1}$. Equation (12) tells us that, when the node density is high, the average watt-per-meter metric approaches its optimal value, i.e., $\bar{H}^* \simeq \eta^*$ for large λ. If we examine Eqs. (4) and (5), we can conclude that $\bar{H}^* \propto \beta^{1/\alpha}$ when the receiver overhead p_{rx} is small and λ is large. We also observe that the receiver overhead has an effect on r^*, the optimal relay distance, only when it is larger than $(\alpha - 1)\, p_{\min}$.

B. Numerical Example

In Subsection III.B, we provide a numerical example. We select large-scale path loss of the radio channel with an exponent value between 2.5 and 4.5, as shown by near-ground channel measurement experiments [2,3]. We assume at the close-in reference distance of 1 meter that the transmitter power required for reliable communication is −80 dBW. This will give us a transmission range of about 110.7 meters at 1.5 watts for fourth-power loss. Data reception requires fixed power consumption at 100 mW, and the transmitter has an adjustable power setting starting from a minimum level of −40 dBW.

Figure 2 shows $\eta(r,\phi)$ for $\phi \in [0, \pi/2)$ with a path loss exponent of $\alpha = 4$. Each curve represents a different value of ϕ. As ϕ increases, η increases monotonically. The minimum watt per meter, for each ϕ, is achieved at the same distance r^*, which in our case is 42.7 meters.

Using a numerical method, we can compute the average watt-per-meter metric for different path losses and node densities. Figure 3 shows that, as we increase density, H^* approaches the optimal value, as predicted by Eq. (12). We also see the strong effect of radio path loss. If we assume a transmission rate of 10 kb/s, then we can plot the bit-meter-per-joule metric, i.e., $\left(\tau \bar{H}^*\right)^{-1}$, as shown in Fig. 4.

We can see that in our example a factor of three separates the best bit-meter-per-joule performance between a third- and fourth-power path-loss channel. That means, on average for each unit of energy spend, the third-power path-loss channel can send three times more information over the same distance or the same information over three times the distance than the same radio operating under fourth-power path loss.

C. Geometry of the Relay Zone

The watt-per-meter metric is highly dependent on the geometry of the network, particularly the position of the relay neighbors. If the relay node's position deviates from the optimal location (i.e.,

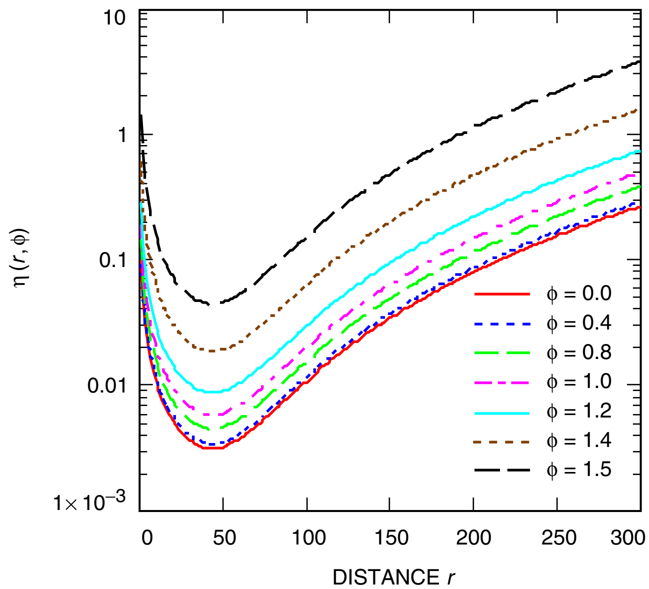

Fig. 2. Watt-per-meter metric as a function of r and ϕ.

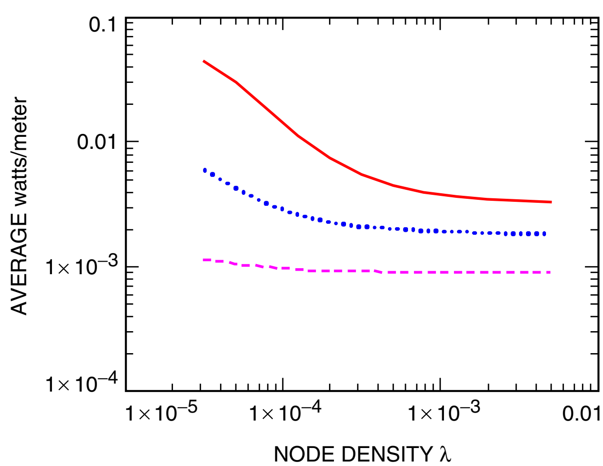

Fig. 3. Average watt-per-meter metric.

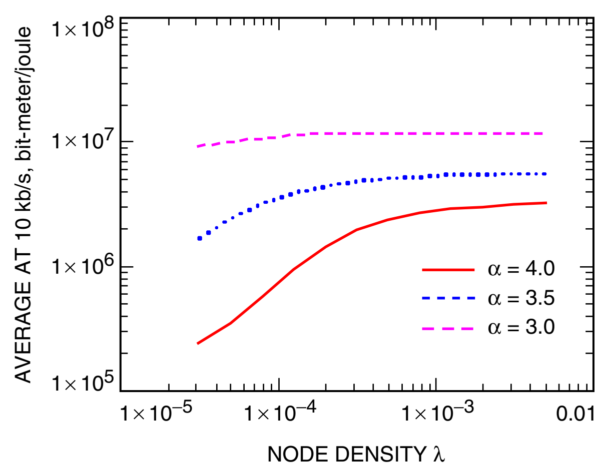

Fig. 4. Average bit-meter-per-joule metric at 10 kb/s.

$R = r^*$ and $\Theta = 0$), we can expect sub-optimal performance (i.e., $E[H^*] > \eta^*$). Two factors control the degree of sensitivity of the watt-per-meter performance to the geometric randomness of the relay nodes: (1) node density and (2) size of the relay zone.

A relay zone represents the region within which a given watt-per-meter performance can be achieved. Having a large relay zone means a system is more tolerant of location deviation than others. Figure 5 shows the geometry of a relay zone for watt-per-meter performance better than or equal to a. The distance to the far-side edge of the boundary is described by $r''(a, (\phi)$; the distance to the near boundary of the zone is given by $r'(a, \phi)$. The maximum angular width of the zone is given by twice the value of $\theta'(a)$. For any given watt-per-meter efficiency, a, the area of the relay zone is given by

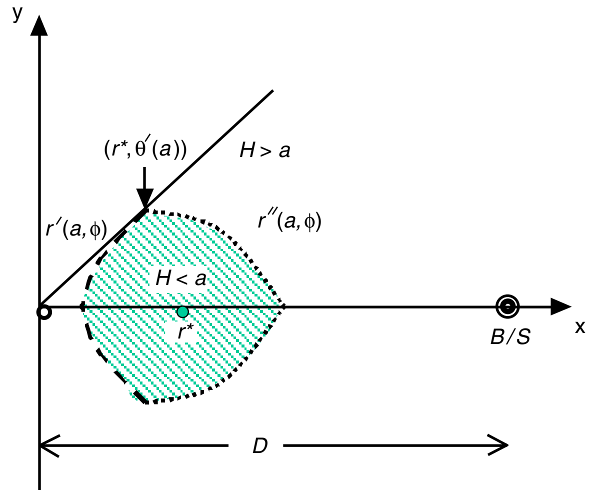

Fig. 5. Relay zone for an adjustable power system.

$$Z(a) = \int_0^{\theta'(a)} \left(r''(a,\phi)^2 - r'(a,\phi)^2 \right) d\phi \tag{13}$$

Then we can computer the average number of relays that can achieve $\eta^* < H < a$,

$$\lambda Z(a) = \lambda \int_0^{\theta'(a)} \left(r''(a,\phi)^2 - r'(a,\phi)^2 \right) d\phi \tag{14}$$

Based on Eq. (12), we can rewrite the expected watt per meter as

$$\bar{H}^* = \eta^* + \int_{\eta^*}^{\infty} e^{-\lambda \cdot Z(a)} da \tag{15}$$

Equation (15) provides an easy geometric interpretation of the average watt-per-meter metric and its relationship to node density and size of the relay zone.

D. Error Analysis

So far we have assumed that D is arbitrarily large to simplify our analysis. This provides us with a far-field result on H^*. However, when D/r^* is a finite value, $r\cos(\theta)$ can become a poor estimate of the net forward progress and produce overly optimistic results.

To derive a bound on the error caused by the simplified calculation of forward-progress distance, we apply some heuristics. First we compute the position of a worst-case equivalent node (i.e., a node with the largest angular deviation possible yet still achieving the same watt-per-meter metric $E[H^*]$ calculated under the far-field assumption). Using this equivalent node, we then compute its watt-per-meter performance using the actual net forward progress given by Eq. (2).

Figure 6 shows the level of under-estimation of the $E[H^*]$ when D/r^* is finite. (Note that for a different path-loss factor α, r^* will change.) As D becomes smaller or the path-loss factor α becomes stronger, the far-field result shows increasing error. For $\alpha = 4$, the far-field result shows a 60 percent possibility of

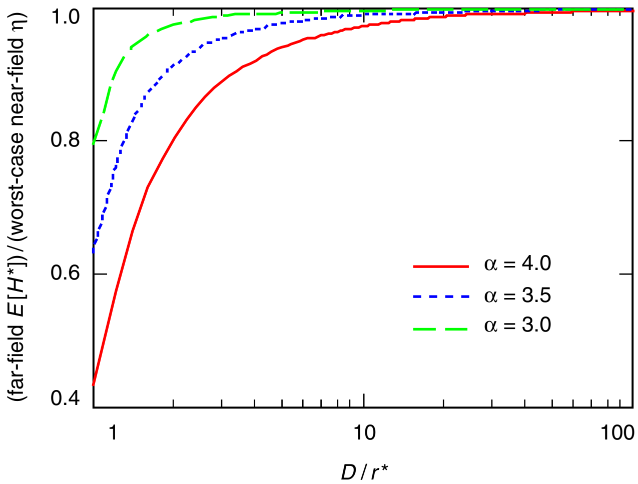

Fig. 6. Worst-case under-estimation of $E[H^*]$ due to error in the net forward progress calculation at finite D/r^*.

error; at twice r^*, the worst-case error is reduced to about 20 percent. As D/r^* increases and path loss lessens, the far-field estimate converges quickly to the actual value.

Note that we plotted only the error for $D/r^* > 1$; this is because if D is equal to or less than r^*, direct communication with the base station is always more advantageous than relay. The error analysis shows us that the far-field average watt-per-meter metric provides a good tool for analyzing large sensor networks because error is bounded within a small area compared to the total region of coverage.

IV. Total Energy Consumption in a Sensor Network

In a space/planetary mission, the prototypical scenario envisioned is a stationary multi-hop sensor network connected to a base-station node, which gathers science data from each sensor. To compute the average cumulative energy consumption in such a scenario, we need to estimate the energy required to relay data from each sensor to a base station through a multi-hop path. We can derive this quantity by multiplying the net distance traversed, i.e., the physical distance between each sensor and the base station, with the watt-per-meter efficiency $\bar{H}^*$ derived from our previous analysis. Let τ represent the transmission time for a single bit of data, and define d to represent the net distance traveled toward the base station; then the joule-per-bit cost over distance d can be estimated by

$$\bar{E}_b(d) \approx \tau \cdot d \cdot \bar{H}^* \quad \text{joules/bit} \tag{16}$$

Given that a sensor network is deployed uniformly within a region S and that it generates a traffic volume of $\rho = \lambda \cdot \mu$ bit/m^2, where λ is the node density and μ is the sensor data-generation volume per node, we can approximate the total energy required to relay all data to a single node located at point $c \in S$:

$$\begin{aligned} E_{\text{total}}(c) &= \int_S \bar{E}_b(|s-c|)\, \rho \cdot ds \\ &= \tau \bar{H}^* \rho \int_S |s-c| \cdot ds \quad \text{joules} \end{aligned} \tag{17}$$

This energy formula can be further generalized to accommodate non-uniform traffic $\rho(s) = \lambda \cdot \mu(s)$ bits/m^2, where the sensor data-generation volume per node depends on the sensor's location. Then we have

$$E_{\text{total}}(c) = \int_S \bar{E}_b(|s-c|)\,\rho(s) \cdot ds$$

$$= \tau \bar{H}^* \lambda \int_S |s-c|\,\mu(s) \cdot ds \quad \text{joules} \tag{18}$$

Note that the relationship between $E_{\text{total}}(c)$ and λ is stronger than linear, because $\bar{H}^*$ itself is a strong function of λ.

A. Analysis of a Sensor Network Deployed in a Square Region

In this subsection, we redefine D as the dimension of the square region covered by a sensor network. The volume of data generated per unit area is $\rho = \lambda\mu$ bits/m^2. Data bits are relayed to a single base station at location (x_c, y_c), as shown in Fig. 7.

The total energy to relay all data can be computed by

$$E_{sqr,D}(x_c, y_c) = \int_{-D/2}^{D/2}\int_{-D/2}^{D/2} \bar{E}_{bm}\left(\sqrt{(x-x_c)^2 + (y-y_c)^2}\right) \cdot \rho \cdot dx \cdot dy$$

$$= \int_{-D/2-y_c}^{D/2-y_c}\int_{-D/2-x_c}^{D-x_c} \bar{E}_{bm}\left(\sqrt{x^2+y^2}\right) \cdot \rho \cdot dx \cdot dy$$

$$\le \tau \bar{H}^* \rho \int_{-D/2-y_c}^{D/2-y_c}\int_{-D/2-x_c}^{D/2-x_c} \sqrt{x^2+y^2} \cdot dx \cdot dy \tag{19}$$

To simplify notation, let $a_x = -D/2 - x_c$, $b_x = D/2 - x_c$, $a_y = -D/2 - y_c$, and $b_y = D/2 - y_c$. We define a function $F(x, y)$ such that

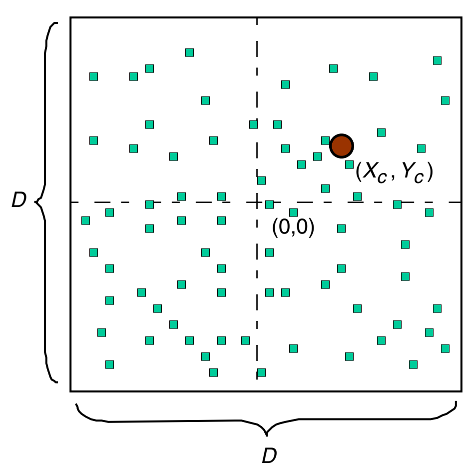

Fig. 7. Sensor network in a square region.

$$F_x(x,y) = \frac{\partial F(x,y)}{\partial x}$$

$$F_y(x,y) = \frac{\partial F(x,y)}{\partial y}$$

$$F_{xy}(x,y) = \frac{\partial^2 F(x,y)}{\partial x \partial y} = \sqrt{x^2+y^2}$$

There is no unique $F(x,y)$, and one possible candidate is the following expression:

$$F(x,y) = -\frac{x^3}{18} + \underbrace{\frac{1}{3}xy\sqrt{x^2+y^2} + \frac{1}{6}y^3 \log\left[x+\sqrt{x^2+y^2}\right] + \frac{1}{6}x^3 \log\left[y+\sqrt{x^2+y^2}\right]}_{\tilde{F}(x,y)=\tilde{F}(y,x)} \tag{20}$$

Then we have

$$\begin{aligned} E_{sqr,D}(x_c,y_c) &\le \tau \bar{H}^* \rho \int_{a_y}^{b_y} \int_{a_x}^{b_x} F_{xy}(x,y) \cdot dx \cdot dy \\ &= \tau \bar{H}^* \rho \int_{a_y}^{b_y} \left[F_y(b_x,y) - F_y(a_x,y)\right] \cdot dy \\ &= \tau \bar{H}^* \rho \left[F(b_x,b_y) - F(a_x,b_y) - F(b_x,a_y) + F(a_x,a_y)\right] \\ &= \tau \bar{H}^* \rho \left[\tilde{F}(b_x,b_y) - \tilde{F}(a_x,b_y) - \tilde{F}(b_x,a_y) + \tilde{F}(a_x,a_y)\right] \end{aligned} \tag{21}$$

In the special case where the base station is in the center of the region, we have $a = a_x = a_y = -D/2$ and $b = b_x = b_y = D/2 = -a$. Then

$$\begin{aligned} E_{sqr,D}(0,0) &= \tau \bar{H}^* \rho \left[\tilde{F}(b,b) - \tilde{F}(-b,b) - \tilde{F}(b,-b) + \tilde{F}(-b,-b)\right] \\ &= \tau \bar{H}^* \rho b^3 \left(\frac{4\sqrt{2}}{3} + \frac{2}{3}\log\left(\frac{\sqrt{2}+1}{\sqrt{2}-1}\right)\right) \\ &= \tau \bar{H}^* \rho D^3 \left(\frac{1}{3\sqrt{2}} + \frac{1}{12}\log\left(\frac{\sqrt{2}+1}{\sqrt{2}-1}\right)\right) \end{aligned} \tag{22}$$

and the average joules/bit is given by

$$E_{\mathrm{bit},D}(0,0) = \frac{E_{sqr,D}(0,0)}{\text{no. of data bits sent} = \rho D^2} = \tau \bar{H}^* D \left(\frac{1}{3\sqrt{2}} + \frac{1}{12}\log\left(\frac{\sqrt{2}+1}{\sqrt{2}-1}\right)\right) \tag{23}$$

Note that the total energy consumption increases as the third power of the dimension of the region, and linearly with the traffic density. If we consider the joules/bit performance, we see the energy efficiency is inversely proportional to the dimension of the square region. Although λ is not an explicit parameter in Eq. (23), its effect is implicit through the average watts/meter metric $\bar{H}^*$.

Back to the calculation of the total energy consumption, let's assume $x_c = y_c = \Delta/\sqrt{2}$, i.e., the base station is at distance Δ meters from the origin and on the diagonal line connecting the origin to the upper-right-hand corner. Let $a = -D/2 - \Delta/\sqrt{2}$ and $b = D/2 - \Delta/\sqrt{2}$. Then the total energy consumption as a function of D and Δ is given by

$$E_{diag}\left(D,\Delta\right) = E_{sqr,D}\left(\frac{\Delta}{\sqrt{2}},\frac{\Delta}{\sqrt{2}}\right) = \tau\bar{H}^*\rho\underbrace{\left[\tilde{F}\left(b,b\right) - 2\tilde{F}\left(a,b\right) + \tilde{F}\left(a,a\right)\right]}_{\sim O(D^3)} \quad \text{joules} \tag{24}$$

B. Case of a Stationary Base Station

We now apply the square region analysis to a single-base-station scenario using specific numeric values for each parameter. We look at both uniform and non-uniform traffic distribution, and also extend the scenario to that of a mobile base station.

1. Uniform Traffic Distribution—A Numerical Example. We assume a transmission rate of 10 kb/s and a path-loss exponent of 4.0. Using the same transceiver parameters as in Subsection III.B, the watt-per-meter performance is 4.218×10^{-3} watts/meter (or, equivalently, 237.08 meters/watt). We assume $\lambda = 545/1\ \text{km}^2$. Each node will send a total of 10^6 bits of data to the base station. We compute the total energy required for relaying data to the base station as a function of the size of the square region; we also look at the total energy increase if the base station is off-center by Δ meters along the diagonal line toward one of the four corners of the region.

Figure 8 shows that on average 8.617 mega-joules are required to relay 13.625 gigabits to the base station, or, equivalently, 6.324×10^{-4} joules/bit. The total energy consumption increases as the third power with respect to D and also is increasing strongly with Δ. If the base station is moved to the corner of the region, then the energy consumption will nearly double to 1.723×10^7 joules—equivalent to having

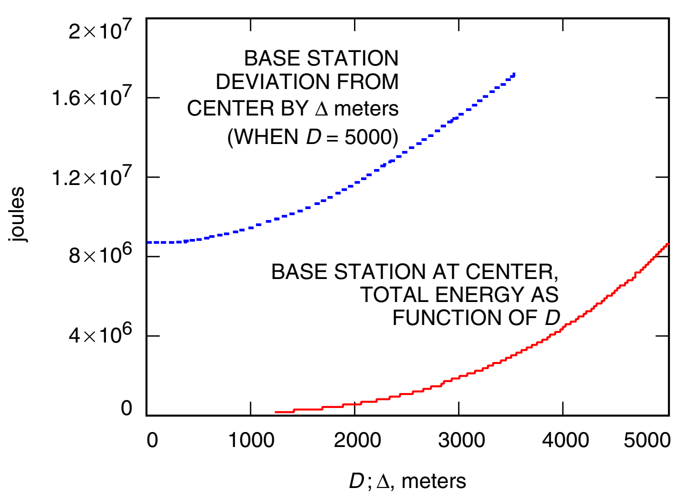

Fig. 8. Effect of network dimension and base-station location on energy.

a network that is 58 percent larger (in terms of physical coverage area, keeping the density fixed) at the same traffic density with a centered base station. In Fig. 9, we plot the total energy consumption as a function of the location of the base station for the same square region. It is clear that the minimum consumption level is achieved when the base station is at the center of the square region.

2. Non-Uniform Traffic Generation. For cases where traffic distribution is non-uniform, adjustment must be made to the base-station location to minimize energy consumption. To study the sensitivity of base-station location to non-uniform traffic, we use a tent-shaped function to model the volume of traffic generated from each node, based on its location:

$$\mu\left(x,y\right) = \frac{10^9}{1+\frac{1}{d_h}\sqrt{\left(x-x_{\text{offset}}\right)^2+y^2}} \quad \text{bits/node} \tag{25}$$

The total traffic volume generated by each node is inversely proportional to its distance from $(x_{\text{offset}}, 0)$, and the maximum is 10^9 bits/node. The parameter d_h is the distance at which the traffic level is reduced by 50 percent. Using the same node density of 545 nodes per square kilometer, we have

$$\rho\left(x,y\right) = \lambda \cdot \mu\left(x,y\right) = \frac{545\times 10^3}{1+\frac{1}{d_h}\sqrt{\left(x-x_{\text{offset}}\right)^2+y^2}} \quad \text{bits/m}^2 \tag{26}$$

Intuitively, we expect the optimal base-station location will be shifted from the center of the square region toward $(x_{\text{offset}}, 0)$. Because no close-form solution is available for a non-constant traffic distribution $\lambda\left(x,y\right)$, numerical integration is applied to compute the optimal base-station location that produces the minimum energy consumption.

We can observe that the optimal base-station position on the x-axis does not shift as much as x_{offset}; in fact, the shift is decreasing percentage-wise as the point of traffic concentration moves farther away from the origin. This is because the relaying cost on the far side of the network also becomes significant as the base station moves further away from the center. Another parameter that can influence the optimal base-station location is d_h, which controls the level of traffic concentration near $(x_{\text{offset}}, 0)$. Larger d_h means less traffic concentration, therefore less base-station movement. In Fig. 10, we see that at $d_h = 5$

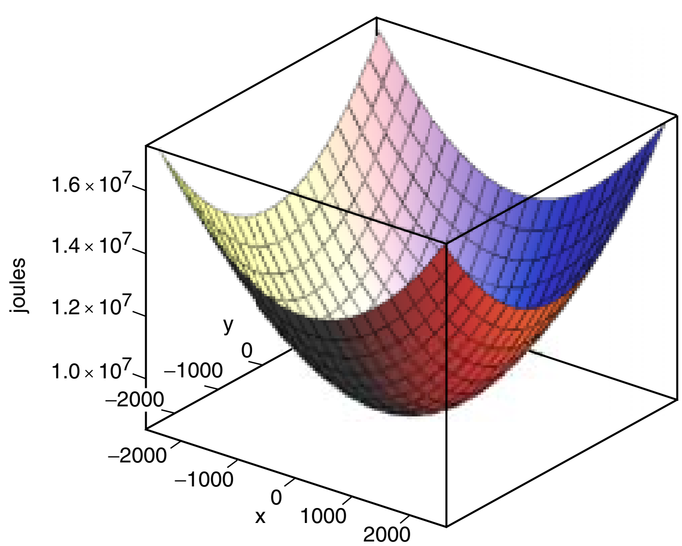

Fig. 9. Total energy (in joules) to collect all sensor data as a function of base-station location.

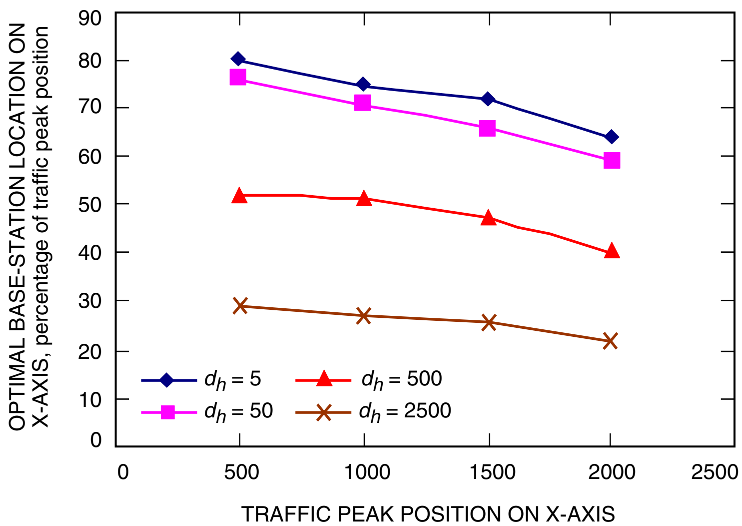

Fig. 10. Sensitivity of the optimal base-station location to traffic distribution.

the base-station movement is between 65 to 80 percent of x_{offset}; for $d_h = 2500$, the base-station movement is only from 22 to 30 percent of x_{offset}. In general, we can say that the optimal base-station location under non-uniform traffic density needs to be adjusted toward the "hot spot." The degree of adjustment depends both on how far the traffic peak location is from the center and on the degree of traffic concentration.

C. Case of a Mobile Base Station

In the last subsection, we have shown that the physical dimension of the network can exercise a strong influence on the total energy consumption. To reduce the adverse effect of a large network, we can partition the network into several smaller sub-networks and use a mobile base station to periodically visit and retrieve data from each sub-network. By allowing the base station to move, we reduced the effective physical dimension of the network while providing the same sensor coverage. As shown in Fig. 11, consider dividing the same D meters-by-D meters region into N^2 equally sized square regions and using a mobile base station to retrieve data from the center of each region. Then the total energy consumption due to radio communication shows an N-fold reduction:

$$\begin{aligned} E_{\text{mobile},N^2}(D) &= N^2 E_{sqr,D/N}(0,0) \\ &= N^2 \tau \bar{H}^* \rho \left(\frac{D}{N}\right)^3 \left(\frac{1}{3\sqrt{2}} + \frac{1}{12}\log\left(\frac{\sqrt{2}+1}{\sqrt{2}-1}\right)\right) \\ &= \frac{E_{sqr,D}(0,0)}{N} \end{aligned} \quad (27)$$

The reduction of transmission energy by a factor of N requires the base station to travel a minimum distance of $N \cdot D$ meters to visit every sub-network. So, we have a trade-off between the cost of base-station mobility and sensor radio communications. While it is probably true that mobility is in general more costly than communications, mobility may be feasible if we can take advantage of the fact that the base station usually carries more energy resources and has the ability to acquire additional energy resources from the environment (i.e., solar or wind power).

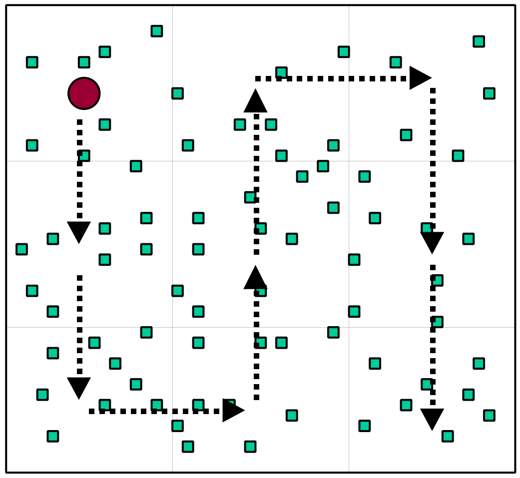

Fig. 11. Partitioned network with mobile base station.

In recent years, a clustering algorithm has been developed to simplify network organization by designating a few nodes as the "cluster head." A cluster-head node functions as the router for nearby sensors and therefore creates a logical partition of the network into small sub-networks called clusters. However, logical partitions, in general, do not reduce the energy consumption because inter-cluster communication is still required to forward data to the base station; there is no net reduction in the average physical distance between each sensor and the base station. Rather, a clustering architecture improves energy efficiency by load balancing [11] and mobility management.

V. Asymmetric Distribution of Energy Consumption

Knowing the total energy consumption allows a simple calculation of average required energy reserve for each sensor. However, due to the asymmetry of traffic flow (i.e., most information converges toward the base station), the actual energy consumption required for each sensor may depend, very significantly, on its distance from the base station. Research in sensor networks has indicated that the performance bottleneck usually is located near the base station, where demand for communication bandwidth and power is highest due to concentration of relay activity.

To compute the asymmetric distribution of energy consumption, we consider, for mathematical convenience, a sensor network deployed within a circular region with diameter D, as shown in Fig. 12, with the base station placed in the center. Let us assume that λ and μ are both constant; then we know that total energy consumption is given by

$$\begin{aligned} E_{cir}(D) &= \rho\tau\bar{H}^* \int_{\{|s-c|\le D/2, c= \text{ origin}\}} |s-c|\, ds \\ &= \rho\tau\bar{H}^* \int_0^{2\pi} \left[\int_0^{D/2} r \cdot r \cdot dr \right] \cdot d\phi \\ &= \rho\tau\bar{H}^* \pi \frac{D^3}{12} \qquad (28) \end{aligned}$$

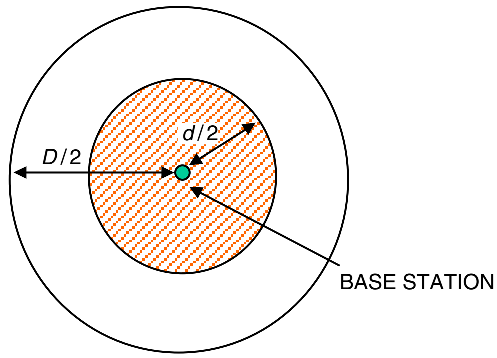

Fig. 12. A sensor network in a circular region.

We can also compute the total energy consumption for a sub-network located within a concentric circle with diameter $d < D$. There are two parts to this computation. The first part accounts for handling data that originated *within* the sub-network; the second part accounts for relaying data that originated from *outside* the sub-network. Thus, we have

$$E_{cir}\left(d, D\right) = \underbrace{\rho\tau\bar{H}^{*}\pi\frac{d^{3}}{12}}_{\substack{\text{energy consumption}\\ \text{incurred by traffic}\\ \text{generated internally}}} + \underbrace{\rho\pi\left(\frac{D^{2}}{4} - \frac{d^{2}}{4}\right)}_{\substack{\text{traffic volume originated}\\ \text{outside the subnetwork}}} \underbrace{\frac{d}{2}}_{\substack{\text{relay}\\ \text{distance}}} \tau\bar{H}^{*}$$

$$= \rho\tau\bar{H}^{*}\pi\left[\frac{D^{2}d}{4} - \frac{d^{3}}{6}\right] \tag{29}$$

We can now compute the average per node energy burden as a function of d:

$$\bar{E}_{\text{node}}\left(d, D\right) = \mu\tau\bar{H}^{*}\left(\frac{D^{2}}{d} - \frac{2d}{3}\right) \tag{30}$$

Let us normalize the localized average per node energy burden $\bar{E}_{\text{node}}(d, D)$ by the global average $\bar{E}_{\text{node}}(D, D)$. Define $\delta = d/D$; then we have

$$\bar{E}_{\text{node\_norm}}\left(\delta\right) = \frac{\bar{E}_{\text{node}}(d, D)}{\bar{E}_{\text{node}}(D, D)} = \left[\frac{3}{\delta} - 2\delta\right], \quad \text{where } \frac{r^{*}}{D} \leq \delta \leq 1 \tag{31}$$

Figure 13 shows the normalized average energy burden for a sub-network whose radius is $\delta \times D$. One can see that there is a pronounced imbalance in energy consumption. For nodes located very close to the base station, the average burden is very high. If we consider the neighbor whose radius is only 1/10 of the radius of the entire area, the energy burden within this small sub-network is 30 times the global average. There is in general a lower limit for $\delta = d/D$, since d represents, at the minimum, the average radius of the 1-hop neighborhood of the base station. A reasonable number to choose for the minimum d would be r^{*}.

Several strategies can be used to handle the imbalance of energy consumption among the sensor nodes. The simplest approach is to increase node density or provision more energy resources per sensor near the

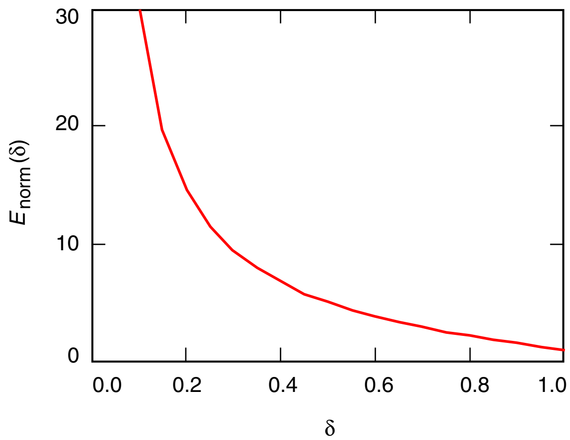

Fig. 13. Normalized average per node energy burden for sub-networks with δ = *d* / *D*.

base station. If mobility is an option, intelligent movement of the base station also can balance energy consumption. Another possibility is to actively shape the traffic volume near the base station by either filtering out redundant information or compressing data as they are relayed closer to the base station.

VI. Conclusion

We have presented a system-level performance characterization of the energy consumption for ad hoc wireless sensor networks. We began by defining the routing, channel, and transceiver power model appropriate in the application domain of a wireless sensor network using radio frequency (RF)-based communication technology. We then derived the bit-meter-per-joule metric over a single radio link. The bit-meter-per-joule metric was then applied to obtain a macro-scale approximation of the total energy consumption required by a sensor network based on the physical coverage, the location of the base station, the node density, and the traffic-generation volume. We specifically looked at the performance of a sensor network deployed in a square region with a single stationary or mobile base station. We made the following observations regarding energy-efficient sensor network operation:

(1) The optimal relay distance is controlled by the trade-off between the propagation path loss and the fixed energy overhead for operating the transceiver. Under adverse channel conditions, a watt-per-meter metric favors short relays; thus, high node density is required.

(2) The optimal base-station location is near the center of the network if the traffic distribution is uniform; otherwise, it tends to shift toward the location where traffic is most concentrated—the degree of shift depends on the degree of traffic concentration and its peak location.

(3) If the base station is mobile, using small clusters or sub-networks of sensors rather than one large connected network can reduce communication cost while providing sensor coverage over the same physical area. However, the base station will pick up the additional cost of mobility.

(4) The average energy consumption is much higher for sensors located near the base station than for those on the outer edge of the network. This imbalance can adversely affect the connectivity and operation lifetime of the network. Techniques such as preferential resource provisioning (i.e., increasing node density or increasing energy resources near the base station), network partitioning (using a mobile base station to visit each sub-network sequentially), and information aggregation and compression can help offset such an imbalance.

References

[1] W. Beyer, *Standard Math Tables*, 28th Edition, Boca Raton, Florida: CRC Press, Inc., 1987.

[2] R. Foran, T. Welch, and M. J. Walker, "Very Near Ground Radio Frequency Propagation Measurements and Analysis for Military Applications," *MILCOM 1999*, vol. 1, pp. 336–40, October 1999.

[3] K. Sohrabi, B. Manriquez, and G. Pottie, "Near Ground Wideband Channel Measurement in 800-1000 MHz," *Proceedings of IEEE Vehicular Technology Conference*, Amsterdam, The Netherlands, pp. 571–574, September 1999.

[4] V. Ailawadhi, J. Gao, G. Pottie, and K. Sohrabi, "Protocols for Self-Organization of a Wireless Sensor Network," *IEEE Personal Communications*, vol. 7, pp. 16–27, October 2000.

[5] S. Singh, M. Woo, and C. S. Raghavendra, "Power-Aware Routing in Mobile Ad Hoc Networks," *MOBICOM'98*, Dallas, Texas, pp. 181–190, October 1998.

[6] H. Takagi and L. Kleinrock, "Optimal Transmission Ranges for Randomly Distributed Packet Radio Terminals," *IEEE Transactions on Communications*, vol. 3, no. 3, pp. 246–257, 1984.

[7] K. Quirk, M. Srinivasan, and J. Agre, "Cooperative Modulation Techniques for Long Haul Relay in Sensor Networks," Global Telecommunications Conference, 2001, *GLOBECOM '01*, IEEE, vol. 2, pp. 1171–1175, 2001.

[8] R. Jain, A. Puri, and R. Sengupta, "Geographical Routing Using Partial Information for Wireless Ad Hoc Networks," *IEEE Personal Communications*, vol. 8, issue 1, pp. 48–57, February 2001.

[9] Z. J. Haas and M. R. Pearlman, "The Performance of Query Control Schemes for the Zone Routing Protocol," *IEEE/ACM Transactions on Networking*, vol. 9, issue 4, pp. 427–438, August 2001.

[10] K. Yao, R. E. Hudson, C. W. Reed, D. Chen, and F. Lorenzelli, "Blind Beam-Forming on a Randomly Distributed Sensor Array System," *IEEE Journal On Selected Areas in Communications*, vol. 16, no. 8, pp. 1555–1567, October 1998.

[11] X. Hong, M. Gerla, H. Wang, and L. Clare, "Load Balanced, Energy-Aware Communications for Mars Sensor Networks," *Proceedings of IEEE Aerospace 2002*, Big Sky, Montana, March 2002.